Vol. 14(4), pp. 110-122, October-December, 2022
DOI: 10.5897/IJWREE2021.1025
Article Number: 160773169855
ISSN: 2141-6613

http://www.academicjournals.org/IJWREE

ACADEMIC JOURNALS
expand your knowledge

International Journal of Water Resources and Environmental Engineering

Full Length Research Paper

Modelling daily river discharge using stochastic differential equation in Ouémé at Savè Basin, Benin, West Africa

Alamou Adéchina Eric[2], Moussa Djibril Aliou[1], Biao Iboukoun Eliézer[1,2]*, Gohouede Lionel Cédric[1] and Obada Ezéchiel[2]

[1]Ecole Nationale Supérieure de Génie Mathématique et Modélisation (ENSGMM/UNSTIM), Abomey, Benin.
[2]Laboratoire de Géosciences de l'Environnement et Applications, Université Nationale des Sciences, Technologies, Ingénierie et Mathématiques (UNSTIM), Abomey, Benin.

Received 24 December, 2021; Accepted 21 April, 2022

This work aims to study the uncertainties in the rainfall-runoff process using a stochastic approach derived from the deterministic hydrological model based on the least action principle (ModHyPMA). The stochastic formulation of ModHyPMA allows for consideration of both the dynamics and stochastic nature of the hydrological phenomenon. The main assumption is that uncertainties in the hydrological process are modelled as Gaussian white noise. It is assumed that hydrological systems are nonlinear dynamical systems that can be described by stochastic differential equations (SDE). From this SDE, we deduce the associated Fokker-Planck equation (FPE). The FPE is a partial differential equation that cannot be solved analytically due to its complexity. We therefore investigated a numerical solution to this equation by using the finite differences and finite volumes methods. The results show that the stochastic model improves the simulations of discharges in Ouémé at Savè Basin (NSE = 0.89, R^2 = 0.90, RMSE = 113 and MAE = 76) compared to the deterministic model (NSE = 0.78, R^2 = 0.78, RMSE = 123 and MAE = 51). The plots of the solutions (the density probability of discharges) always coincide when the investigated numerical solutions are compared, except when the number of meshes is very small (100 meshes). The two solutions are convergent. This numerical solution provides information about the distribution of discharges in the Ouémé at Savè Basin.

Key words: Uncertainty, stochastic approach, Fokker-Planck equation (FPE), ModHyPMA, numerical solutions, density probability.

INTRODUCTION

There is much evidence nowadays that the planet is warming up, largely as a result of human generated greenhouse gases (Kundzewicz et al., 2014; IPCC 2014a, b). Extreme hydrological phenomena such as floods and droughts are caused by the acceleration of climate variability. Benin, like all West African

*Corresponding author. E-mail: biaoeliezer@yahoo.fr

countries, has been experiencing increasing climate fluctuations since 1970 (Sintondji et al., 2014). Thus, all sectors depending on water availability (such as agriculture, water supply, hydroelectricity, etc) are now highly vulnerable to the effects of climate change. This situation has prompted hydrologists to question the existing rainfall-runoff modelling methods, and several modelling attempts aim to contribute more effectively to the reduction of uncertainties associated with the assessment of the impacts of climate variability and changes on water resources. As a result, we require an approach that can account for both the dynamics and the random nature of the physical phenomenon.

Mathematically, stochastic systems can be modelled by stochastic differential equation (SDE) in the time continuous case (Zorzano et al., 1999). In the following, we will restrict our considerations to SDE with Gaussian white noise. In many problems, Gaussian white noise has been used as an approximation of the stochastic term. (Pauluhn, 1993). The solution of this SDE is the Markovian diffusion process. One of the most important advantages of the SDE is the associated Fokker-Planck equation (FPE), which allows one to directly derive the time-varying probabilities associated with the outflow (Biao et al., 2016). The FPE models the time evolution of the probability distribution in a system under uncertainty. The major problem for the FPE is that this equation does not have an explicit solution. It can be solved numerically or by approximation using orthogonal polynomials. Alamou (2011) and Biao et al. (2016) used the Hermite polynomial expansion to approximate the exact solution of the FPE. To the best of our knowledge, no study has so far investigated the numerical resolution of the FPE in our study area, even in West Africa; none have investigated the time evolution of the density probability function of the river discharges. The present study fills this gap.

The objective of this paper is, therefore, to consider the uncertainties in the rainfall-runoff modelling. The deterministic hydrological model based on the least action principle (ModHyPMA) is compared with its stochastic model in terms of simulations of discharges. Finite differences and finites volumes methods are among the other methods that have been widely used to numerically solve the FPE. A successful approach to overcoming the limitations of simple finite differences is achieved by Wojtkiewiczet et al. (1999) in terms of higher order finite differences. Thus, the time-dependent probability distribution for the resulting discharge is obtained in the form of the numerical methods of finite differences of higher order (order 4) and finite volumes.

METHODOLOGY

Study area and data used

The Ouémé at Savè catchment stretches out from the center to the North of Benin between 7° 58-10° 12 N and 1° 35- 3° 05 E (Figure 1). It covers an area of 23,600 km^2 (Le Barbe et al., 1993) which is about 47.2% of the whole Ouémé catchment. On a global view, Benin extends from the Niger River to the Atlantic Ocean, with a relatively flat terrain, small mountains (about 600 m), and low coastal plains with marshlands, lakes, and lagoons. The study area has a unimodal rainfall season (from mid March to October) that peaks in August. The interannual mean rainfall is around 1075 mm; the minimum is 680 mm (in 1983), and the maximum is 1693 mm (in 1963). The Ouémé catchment landscape is characterized by gallery forest, savannah, woodlands, agricultural lands, pastures and mosaics of cropland and bush fallow, plantation with parkia, cashew, and palm trees (Bossa, 2007). In the Ouémé catchment, the main landscape elements are the crest and the upper, middle, and lower slopes (together referred to high peneplains), followed by the valley fringe and colluvial footslopes, and the valley bottoms and terraces (low peneplains and floodplains) (Igué et al, 2000).

Data used in this study consist of daily rainfall data, daily potential evapotranspiration (ETP), and daily discharge data. Rainfall and ETP data were provided by Meteo-Benin, while discharge data were provided by the National Directorate of Water (DG-Eau Benin). The period 1961 - 2010 has been chosen as the study period (good compromise, taking into account the length of the data available in the different stations). Spatialized regional daily mean rainfall was obtained by kriging (Matheron, 1970) with an exponential variogram.

ModHyPMA Model description

The hydrological model based on the least action principle (ModHyPMA) is described by Afouda et al. (2004), Afouda and Alamou (2010), Alamou (2011) and Biao et al. (2016) as follows:

$$\frac{dZ}{dt} = \psi(q,t) \tag{1}$$

$$\frac{d(\lambda Q)}{dt} + \mu Q^{2\mu-1} = \psi(q,t) \Rightarrow \frac{dQ}{dt} = Y(Q,\psi,\lambda) \tag{2}$$

Where:
Z describes the variation of the initial state of the catchment,
ψ describes the model input,
Y describes the model structure,
λ and μ are the physical parameters of the model, and
Q stands for the river discharge.

Equation 1 describes explicitly the production process (that is, the action of the unsaturated zone that accounts for evaporation and evapotranspiration, and divides the resulting rainfall event into two components: overland and underground) and Equation 2 describes the transformation process (that is, the process by which the rainfall volumes for the overland component and the underground component are transformed into runoff) (Alamou, 2011). The scheme and main equations of the deterministic ModHyPMA are given in Figure 2.

Stochastic differential equation describing the River Basin and its associated Fokker-Planck equation

To account for the different types of uncertainties (that is, uncertainties related to our imperfect knowledge of the physical phenomenon and uncertainties related to the quantitative evaluation of the parameters of the environment, particularly rainfall), the stochastic formulation of ModHyPMA is derived from its

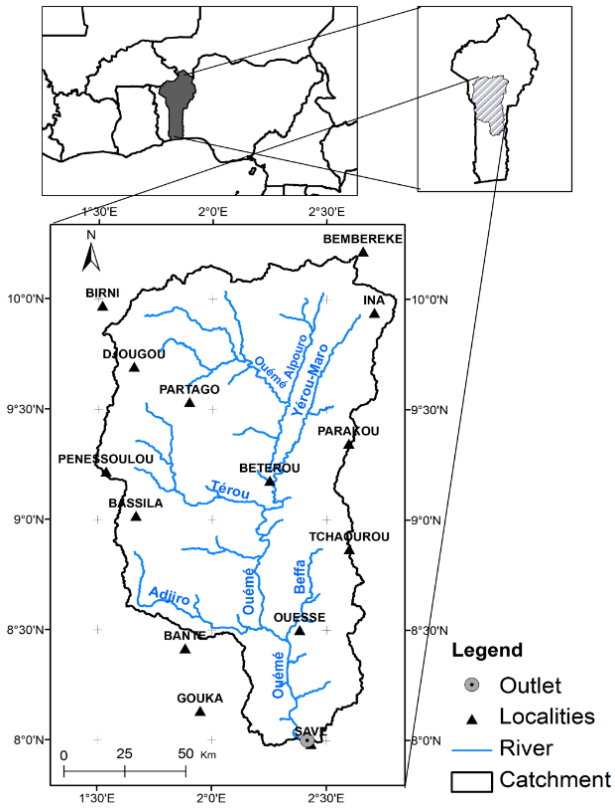

Figure 1. Geographical location of Ouémé at Savè catchment.

foundation in the SDE, which has already been successfully applied in a wide range of hydrological applications. From Equation 2 we can derive Equation 3 as :

$$Y(Q,\psi,\lambda) - \frac{\mu}{\lambda}Q^{2\mu-1} + \frac{1}{\lambda}\psi(q,t) \tag{3}$$

Let us focus on Equation 2, $\frac{dQ}{dt} = Y(Q,\psi,\lambda)$

$\frac{dQ}{dt}$ is the variation of discharge Q with respect to time. In the case of daily discharge, this variation can be written in the form of ΔQ which represents the variation of discharge from day t to day $t + \Delta t$, with Δt = 1day. Let us now model the uncertainties by a Gaussian white noise process r_t which can be added to the structure of the deterministic model Y. The stochastic process represents the variation $\frac{dQ}{dt}$ which is therefore given by $Y_t = \hat{Y}_t + r_t$ with $\hat{Y}_t = -\frac{\mu}{\lambda}Q^{2\mu-1} + \frac{1}{\lambda}\psi(q,t)$. We will now continue the reasoning with the process,

$$\varepsilon_{\,t} = \frac{r_t - \bar{r}}{\sigma_r} \tag{4}$$

which is also a Gaussian white noise, with $\bar{r} = E[r]$ and σ_r representing the intensity of the noise.

For simplicity, let us set $R = \bar{r}$ and $G = \sigma_r$. Equation 4 reads,

$$r_t = R + G.\ \varepsilon_{\,t} \tag{5}$$

By replacing the expression of $\hat{Y}_t$ and r_t , Y_t becomes:

$$Y_t = -\frac{\mu}{\lambda}Q^{2\mu-1} + \frac{1}{\lambda}\psi(q,t) + R + G.\ \varepsilon_{\,t} \tag{6}$$

The question which arises now is to find the values of the constants R and G. To this end, we can deduce that,

$$r_t = \frac{dQ}{dt} - \hat{Y}_t = \frac{dQ}{dt} + \frac{\mu}{\lambda}Q^{2\mu-1} - \frac{1}{\lambda}\psi(q,t) \tag{7}$$

This process r_t can be seen as the residuals from the approximation of $\frac{dQ}{dt}$ by the deterministic model ModHyPMA. Therefore, $\frac{dQ}{dt}$ can be obtained from the observed data using:

$$\Delta Q = Q_t - Q_{t-1} \tag{8}$$

Thus, the estimators of R and G are given in the form:

$$R = E\left[\frac{dQ}{dt} + \frac{\mu}{\lambda}Q^{2\mu-1} - \frac{1}{\lambda}\psi(q,t)\right] \tag{9}$$

$$G^2 = Var\left[\frac{dQ}{dt} + \frac{\mu}{\lambda}Q^{2\mu-1} - \frac{1}{\lambda}\psi(q,t)\right] \tag{10}$$

Let us set, $f(Q,t) = -\frac{\mu}{\lambda}Q^{2\mu-1} + \frac{1}{\lambda}\psi(q,t) + R$ (11)

Thus, $Y_t = \frac{dQ}{dt} = f(Q,t) + G.\ \varepsilon\,(t)$ (12)

Equation12 can be written in the form,

$$dQ = f(Q,t)dt + G.\ \varepsilon\,(t)dt \tag{13}$$

The Gaussian white noise $\varepsilon(t)$ can be described as the formal derivative in time of a Wiener process, W(t), i.e. dW(t) = ε(t)dt. Therefore, the SDE that describes the River Basin is given by Equation 14.

$$dQ = f(Q,t)dt + G.dW(t), \quad Q(t_o) = Q_0 \tag{14}$$

The FPE that is associated with the SDE describing the River Basin is (Risken, 1989):

$$\frac{\partial P(Q,t)}{\partial t} = -\frac{\partial}{\partial Q}[f(Q,t)P(Q,t)] + \frac{1}{2}\frac{\partial^2}{\partial Q^2}(G^2P) \tag{15}$$

with the initial conditions,

$$P(Q,t)|_{t=t_0} = \delta(Q - Q_0) = \begin{cases} 1, & si\ Q = Q_0 \\ 0 & si\ \ Q \neq Q_0 \end{cases} \tag{16}$$

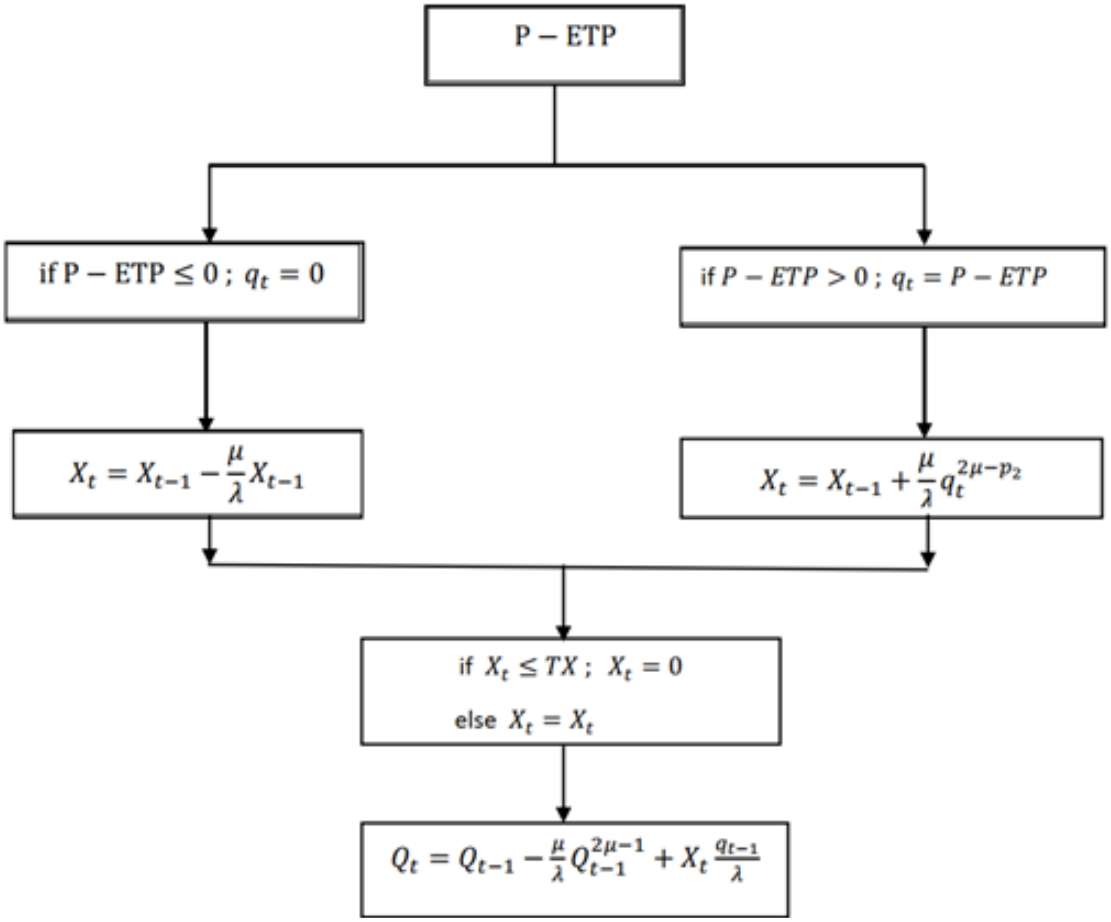

Figure 2. Scheme and main equations of the deterministic ModHyPMA.

And the absorbing limit conditions,

$$P(Q_{min}, t) = P(Q_{max}, t) = 0 \quad (17)$$

Numerical approximation of the solution of the stochastic differential equation (SDE): Euler Scheme

The numerical Euler Scheme to the SDE given in Equation 14) is:

$$Q_{t+\Delta t} = Q_t + f(Q,t)\Delta t + G.(W_{t+\Delta t} - W_t), \qquad Q_{t_0} = Q_0 \quad (18)$$

with $W_{t+\Delta t} - W_t = \Delta W_t \sim N(0,1)$ and $\Delta t = 1\ day$.

The scheme and the main equations of our stochastic approach are summarized in Figure 3.

Model performance criteria

To evaluate the model performance for calibration, the following criteria were taken into account: the Nash-Sutcliffe Efficiency (NSE) (Nash and Sutcliff, 1970), the coefficient of determination (R^2), the root mean square error (RMSE) and the mean absolute error (MAE). The Nash-Sutcliffe Efficiency is defined as:

$$NSE = 1 - \frac{\sum_{i=1}^{n}\left(Q_{obs}(i) - Q_{sim}(i)\right)^2}{\sum_{i=1}^{n}(Q_{obs}(i) - \bar{Q}_{obs})^2} \quad (19)$$

where $Q_{obs}(i)$, $Q_{sim}(i)$, and $\bar{Q}_{obs}(i)$ stand, respectively for the observed discharge, simulated discharge, and the arithmetic mean of Q_{obs} for all events, i = 1 to n. The NSE can attain values from -1 to 1. The value of 1 indicates the total agreement of observed and simulated discharges. An efficiency of 0 (NSE = 0) indicates that the model predictions are as accurate as the mean of observed data; whereas an efficiency less than zero (NSE < 0) occurs when the observed mean is a better prediction than the model; in other words, when the residual variance is larger than the data variance. Essentially, the closer the model is to 1, the more accurate the model is. The coefficient of determination is a number that indicates how well a data fits a statistical model, sometimes simply a line or curve. The coefficient of determination ranges from 0 to 1. An R^2 of 1 indicates that the regression line perfectly fits the data. The RMSE represents the average distance between the simulated and observed data,

$$RMSE = \sqrt{\frac{1}{n}\sum_{i=1}^{n}\left(Q_{obs}(i) - Q_{sim}(i)\right)^2} \quad (20)$$

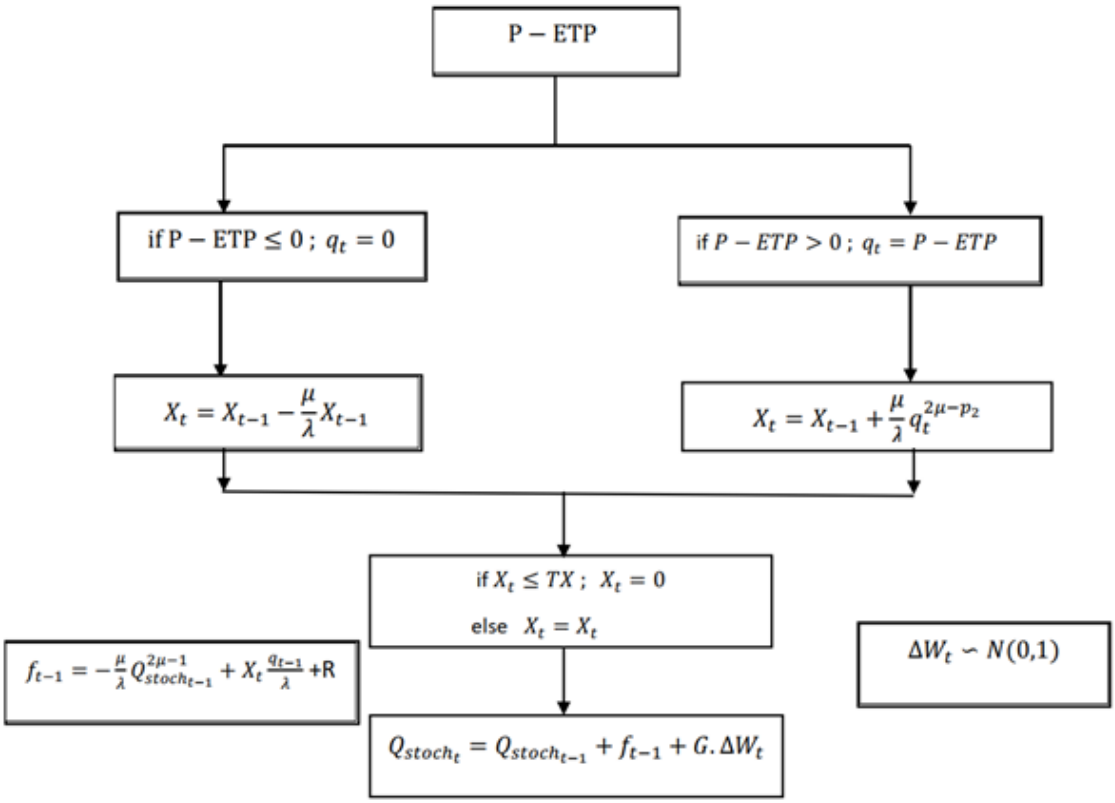

Figure 3. Scheme and main equations of the stochastic model.

$$MAE = \frac{1}{n}\sum_{i=1}^{n} |Q_{obs}(i) - Q_{sim}(i)| \quad (21)$$

Numerical solution of the Fokker-Planck equation using the finite difference of high order 4 and finite volume methods

Finite difference method

In numerical analysis, finite-difference methods are a class of numerical techniques for solving differential equations by approximating derivatives with finite differences. Today, finite-difference methods are one of the most common approaches to the numerical solution of partial derivative equations, along with finite element methods (Grossmann et al., 2007). The higher the order of the finite difference method, the greater the accuracy of the numerical solution. This is the reason for chosing the finite differences of order 4 for solving the FPE. The procedure used in solving boundary problems by finite difference method is as follows: (1) Building the domain mesh; (2) Transforming the partial derivative equation into a numerical finite difference scheme; (3) Writing the finite difference equation at the mesh points; (4) Obtaining the system of discrete algebraic equations and (5) Finding the solution by solving the system of equations.

i. **Decomposition of the domain in elementary meshes:** The spatio-temporal domain W is built according to the following relations:

m subdivisions along the Q axis ; $Q_{max} = Q_{min} + m\Delta Q$

Along the time axis, we used the step Δt and we have:

$$t_j = t_0 + j\Delta t \;\; avec\, j \in \mathbb{N}, \;\; \Delta t = 1\, day$$
$$t_j = t_0 + j \;\; avec \;\; j \in \mathbb{N}$$

We have $P(Q_i, t_j) = P(Q_{min} + i\Delta Q, \;\; t_0 + j\Delta t) = P_{i,j}$
The limits conditions : $P_{0,j} = P_{m,j} = 0, \;\; \forall j \in \mathbb{N}$.
The initial conditions : $P_{i,0} = \delta(Q_i - Q_0)$
$\forall i = 1{:}\, m-1, \quad P_{i,0} = 1$ if $Q_{i-1} < Q_0 < Q_i$ and $P_{i,0} = 0$ otherwise.
In the particular case where $Q_0 = Q_{min}$, we have $P_{i,0} = 1$ and $P_{i,0} = 0$ for i=2: m-1
Q_{max} is always chosen so that Q_0 does not belong to the interval $[Q_{m-1}, Q_m]$.

ii. **Numerical scheme of the finite differences of the partial derivative equation:** We used the finite difference scheme of order 4 for the first and second derivatives of P(Q, t) with respect to Q and the backward scheme of order 1 for the first derivative P(Q, t) with respect to t. The choice of the backward scheme for the first derivative of P(Q, t) with respect to t is due to the fact that it leads to an implicit scheme that is always stable.

iii. **Finite difference equation at mesh points:** At each fixed date $j \geq 1$, the index i must be varied between 1 and m - 1 in order to write the finite difference equations at m – 1 mesh points. We have to solve, for each given j, a system of m - 1 equations with m - 1 unknowns.

iv. **System of discrete algebraic equations:** Before finding the

discrete solutions to the equation at any date j, we have to find all the solutions up to j - 1 since we need information up to this order. Therefore, the numerical solution of our problem must begin with the resolution of the system obtained at j = 1. The system of equations is given by:

$$(S_1):\underbrace{\begin{pmatrix} C_1 & D_1 & E_1 & 0 & 0 & \dots & 0 \\ B_1 & C_1 & D_1 & E_1 & 0 & \ddots & \vdots \\ A_1 & B_1 & C_1 & D_1 & E_1 & \ddots & 0 \\ \vdots & \ddots & \ddots & \ddots & \ddots & \ddots & 0 \\ 0 & \ddots & A_1 & B_1 & C_1 & D_1 & E_1 \\ \vdots & \ddots & 0 & A_1 & B_1 & C_1 & D_1 \\ 0 & \dots & 0 & 0 & A_1 & B_1 & C_1 \end{pmatrix}}_{[M_1]} \underbrace{\begin{pmatrix} P_{1,1} \\ P_{2,1} \\ \vdots \\ P_{i,1} \\ \vdots \\ P_{m-2,1} \\ P_{m-1,1} \end{pmatrix}}_{\{Y_1\}} = r \underbrace{\begin{pmatrix} P_{1,0} \\ P_{2,0} \\ \vdots \\ P_{i,0} \\ \vdots \\ P_{m-2,0} \\ P_{m-1,0} \end{pmatrix}}_{r\{Y_0\}} \quad (22)$$

The system to be solved for j = 1 is therefore $\{S_1\}$: $M_1 Y_1 = r Y_0$. The system to be solved at date j is therefore the following:

$$(S_j):\underbrace{\begin{pmatrix} C_j & D_j & E_j & 0 & 0 & \dots & 0 \\ B_j & C_j & D_j & E_j & 0 & \ddots & \vdots \\ A_j & B_j & C_j & D_1 & E_j & \ddots & 0 \\ \vdots & \ddots & \ddots & \ddots & \ddots & \ddots & 0 \\ 0 & \ddots & A_j & B_j & C_j & D_j & E_j \\ \vdots & \ddots & 0 & A_j & B_j & C_j & D_j \\ 0 & \dots & 0 & 0 & A_j & B_j & C_j \end{pmatrix}}_{[M_j]} \underbrace{\begin{pmatrix} P_{1,j} \\ P_{2,j} \\ \vdots \\ P_{i,j} \\ \vdots \\ P_{m-2,j} \\ P_{m-1,j} \end{pmatrix}}_{\{Y_j\}} = r \underbrace{\begin{pmatrix} P_{1,j-1} \\ P_{2,j-1} \\ \vdots \\ P_{i,j-1} \\ \vdots \\ P_{m-2,j-1} \\ P_{m-1,j-1} \end{pmatrix}}_{r\{Y_{j-1}\}} \quad (23)$$

v. **Solving the system of equations:** At each date j, there is a system of equations (Sj) to be solved. For the resolution of the system, direct Gaussian method has been applied.

Finite volume method

The finite volume method is used to represent and evaluate partial differential equations in the form of algebraic equations (LeVeque, 2002). In the finite volume method, volume integrals in a partial differential equation that contains a divergence term are converted to surface integrals using the divergence theorem. Finite volume methods can be compared and contrasted with the finite difference methods, which approximate derivatives using nodal values, or finite element methods, which create local approximations of a solution using local data, and a global approximation constructed by stitching them together. In contrast, a finite volume method evaluates exact expressions for the average value of the solution over some volume and uses these data to construct approximations of the solution within cells (Fallah et al., 2000). At a date t = n, the numerical solution of the problem is obtained by solving the following:

$$(S_n):\underbrace{\begin{pmatrix} D_n & C_n & 0 & 0 & 0 & \dots & 0 \\ A_n & B_n & C_n & 0 & 0 & \ddots & \vdots \\ 0 & A_n & B_n & C_n & 0 & \ddots & 0 \\ \vdots & \ddots & \ddots & \ddots & \ddots & \ddots & 0 \\ 0 & \ddots & 0 & A_n & B_n & C_n & 0 \\ \vdots & \ddots & 0 & 0 & A_n & B_n & C_n \\ 0 & \dots & 0 & 0 & 0 & A_n & E_n \end{pmatrix}}_{[M_n]} \underbrace{\begin{pmatrix} P_1^n \\ P_2^n \\ \vdots \\ P_i^n \\ \vdots \\ P_{m-1}^n \\ P_m^n \end{pmatrix}}_{\{Y_n\}} = \Delta Q^2 \underbrace{\begin{pmatrix} P_1^{n-1} \\ P_2^{n-1} \\ \vdots \\ P_i^{n-1} \\ \vdots \\ P_{m-1}^{n-1} \\ P_m^{n-1} \end{pmatrix}}_{\{Y_{n-1}\}} \quad (24)$$

It is therefore necessary to start from the numerical resolution of the system obtained at n = 1 to find the discrete solutions of the equation at any date n.

RESULTS AND DISCUSSION

Simulation of discharge with deterministic ModHyPMA

The hydrological model has been calibrated over the period 2003 - 2007 and validated over the period 2009 - 2010. Figure 4 shows the result of the simulated hydrograph compared with the observed discharge for the calibration period. Figure 5 presents the same data for the validation period. The difference between the observed and simulated results can be seen by a simple visual control, and the numerical values for NSE, R^2, RMSE and MAE as presented in Table 1. The recession curve is quite well simulated. However, the uncertainties associated with the peaks are greater than those associated with low flow. These findings are in line with Biao et al. (2016). The fact that the discharge peaks are not well simulated can be attributed to data errors (Andréassian et al., 2010; Kuczera et al., 2010). The improper representation of uncertainty is an intrinsic drawback of the deterministic hydrological models since they do not include components that enable the preservation of the associated statistical characteristics of the observed data. For both the calibration and the validation periods, the NSE and R^2 are greater than 0.70 (Table 1), while RMSE of 123 and MAE of 51 for the calibration period and RMSE of 184 and MAE of 90 for the validation period were achieved. These results indicate that ModHyPMA is suitable for the simulation of river discharge in the Ouémé River Basin. However, there are still many sources of uncertainty not being taken into account by ModHyPMA.

Stochastic model

The simulation with the stochastic model has been performed over the period 2009- 2010. Figure 6 shows in the same graph the observed discharge, the simulated discharge with deterministic ModHyPMA, and the simulated discharge with the stochastic model. It can be seen from this figure that the simulated peaks with the stochastic model are much close to the peaks from observed data than the simulated peaks with the deterministic model. The NSE and R^2 are greater than 0.89, while RMSE of 113 and MAE of 76 were achieved.

Numerical solutions of the Fokker-Planck equation

The numerical solutions of the Fokker-Planck equation are the distributions probability of the river discharge. These distributions express the lack of confidence (that

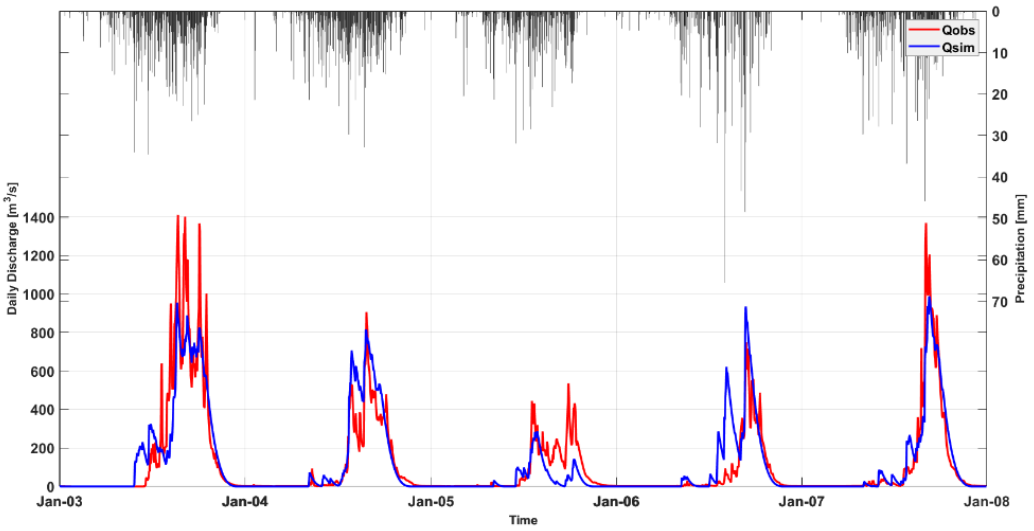

Figure 4. Simulated hydrograph compared with the observed discharge (calibration) for the Savè catchment.

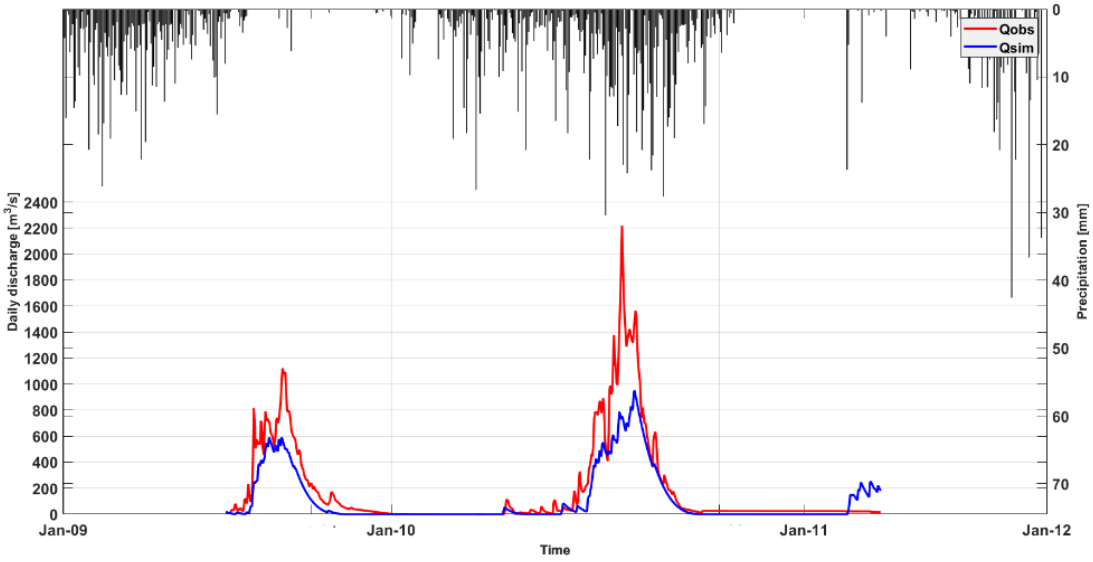

Figure 5. Simulated hydrograph compared with the observed discharge (validation) for the Savè catchment.

Table 1. Performance criteria of ModHyPMA for the Savè catchment, Ouémé River.

Criteria	NSE	R^2	RMSE	MAE
Model calibration (2003-2007)	0.78	0.78	123	51
Model validation (2009-2010)	0.72	0.88	184	90

is, uncertainty) in the real discharge of the days at which one wants to estimate the discharge. We have chosen to solve this equation over 100 days from the date 09/22/2011 (that is, t_0: 09/22/11) with the initially given discharge Q_0 = 553.70 m^3/s. We used the same number of meshes, each time to compare the two investigated

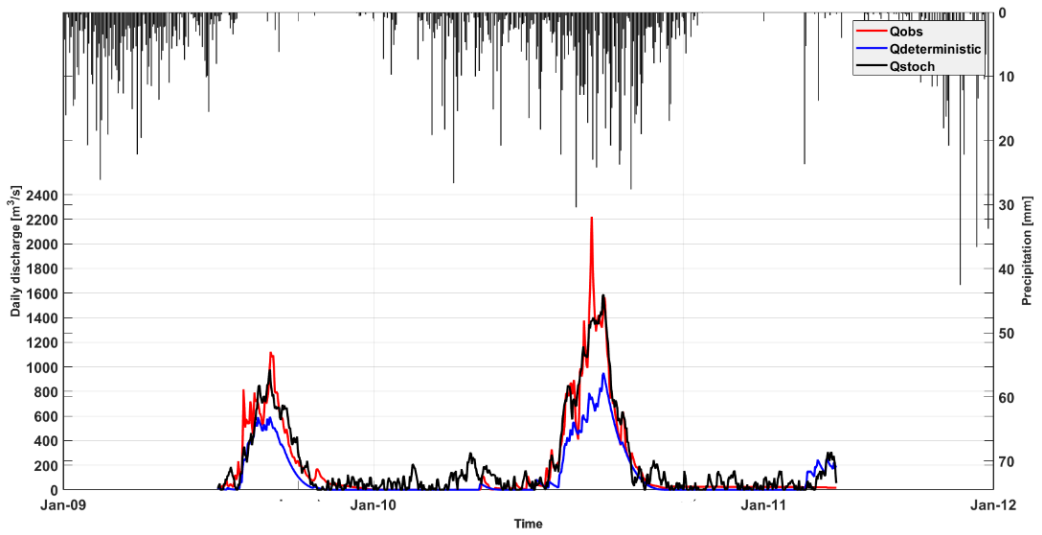

Figure 6. Observed and simulated discharge with deterministic and stochastic ModHyPMA.

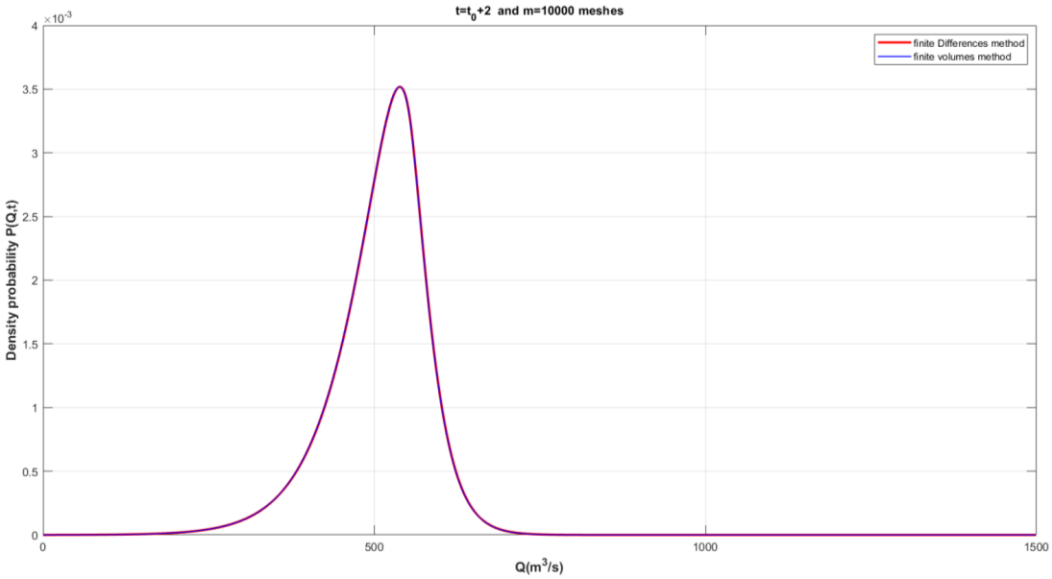

Figure 7. Density probability of discharge derived from the finite difference and finite volumes methods at $t_0 + 2$ days.

numerical methods: the finite differences of order 4 and the finite volume methods. The minimum value of discharge Q is equal to 0 m^3/s and the maximum value Qmax = 5000 m^3/s, a value that cannot be exceeded by the discharge.

Let us start first with m = 10,000 meshes to compare the two methods over 100 days. Figures 7, 8 and 9 show, respectively the numerical solutions of the two methods for days $t_0 + 2$, $t_0 + 20$ and $t_0 + 100$. We have gone to the order of 10^{-4} before it can be noticed that the density probability of the discharge from the finite difference method is hidden by the density probability obtained with the finite volumes approach. From Figure 10, we notice a difference of at most 2.595×10^{-4} - 2.59×10^{-4} = 5 $\times10^{-7}$ between the two peaks. The above results lead us to conclude that the two solutions are convergent for 10,000 meshes. We now reduce the number of meshes to 1000 at $t_0 + 100$ days, and then to 100 to compare the two numerical methods. The results obtained are presented in Figures 11 and 12.

From Figures 11 and 12, the slight difference between the two solutions appears from m = 100 meshes. All

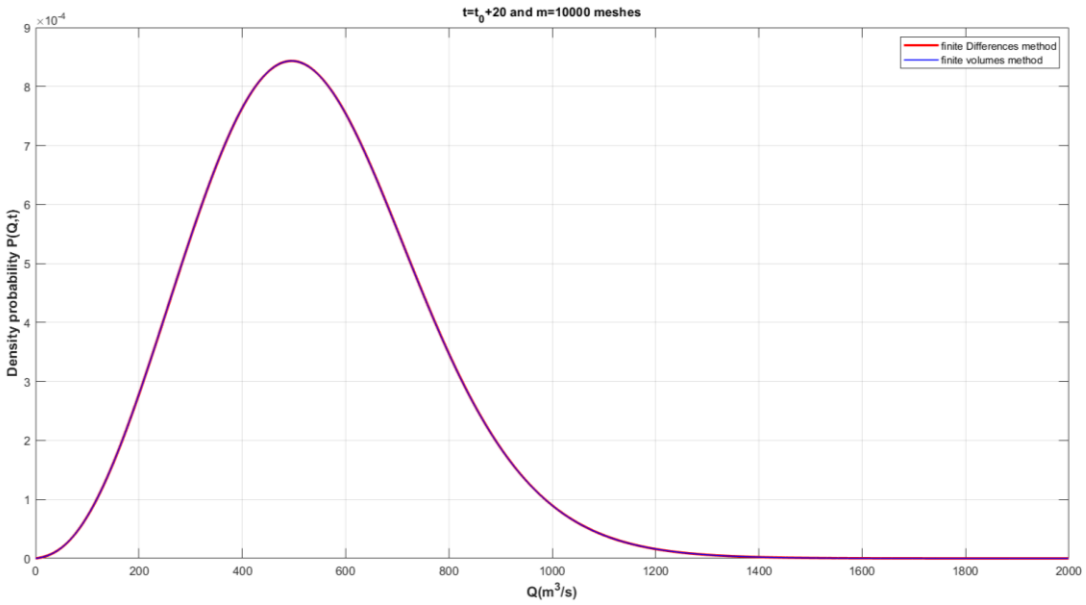

Figure 8. Density probability of discharge derived from the finite difference and finite volumes methods at $t_0 + 20$ days.

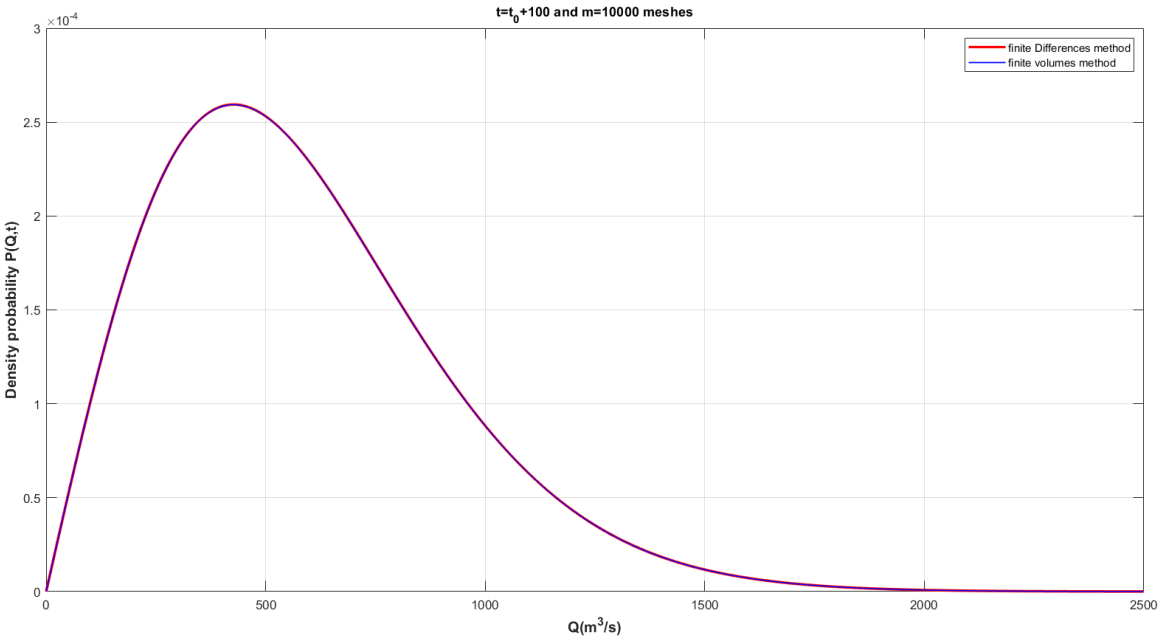

Figure 9. Density probability of discharge derived from the finite difference and finite volumes methods at $t_0 + 100$ days.

these results are satisfactory and allow us to conclude that the two numerical solutions are convergent. We can therefore confirm that the derived density probability of discharge is close to the exact solutions of the FPE. Let us now continue with only the finite difference method and we consider 5,000 meshes. Figure 13 shows the density probability of discharge at some dates ($t_0 + 2$, $t_0 + 10$, $t_0 + 50$ and $t_0 + 100$ days).

It can be seen that the density probability of discharge flattens out and covers more discharges as time evolves. This can be justified by the fact that there are more uncertainties when moving from t_0 to $t_0 + 10$. The further

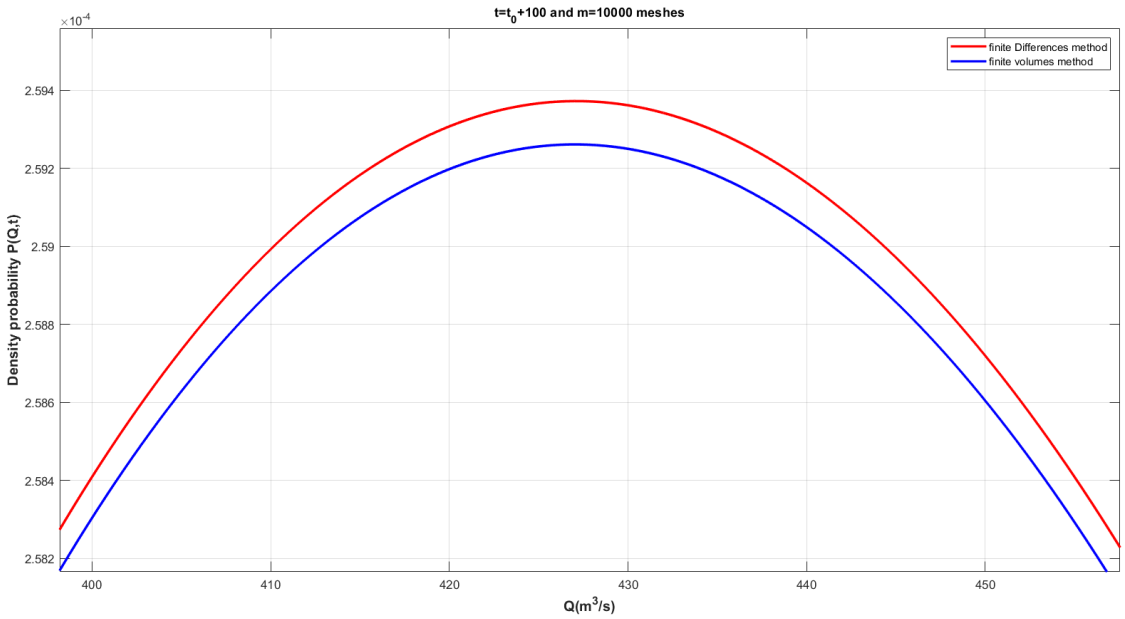

Figure 10. Comparison between the density probability of discharge derived from the finite difference and finite volumes methods at $t_0 + 100$ days.

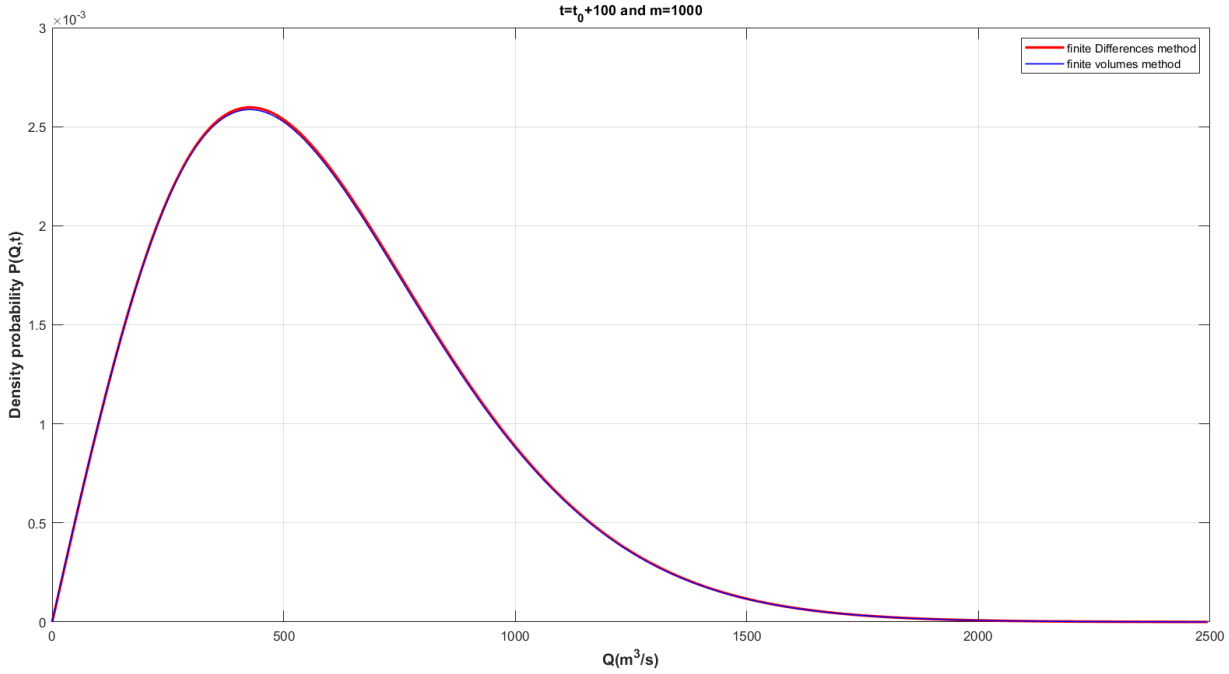

Figure 11. Comparison of the numerical solutions for m = 1000 meshes.

away from t_0, the more there will be uncertainties in the discharge concerning Q_0. Indeed, the solution of the FPE is the density of probability knowing Q (t_0) = Q_0: this is a transition density probability. We also notice that the probability density is symmetric like a normal distribution when it covers an interval that does not contain the boundaries (as in the case $t_0 + 2$); this is due to the Gaussian white noise hypothesis we made at the beginning. However, the densities probability become asymmetric when they cover an interval containing one of

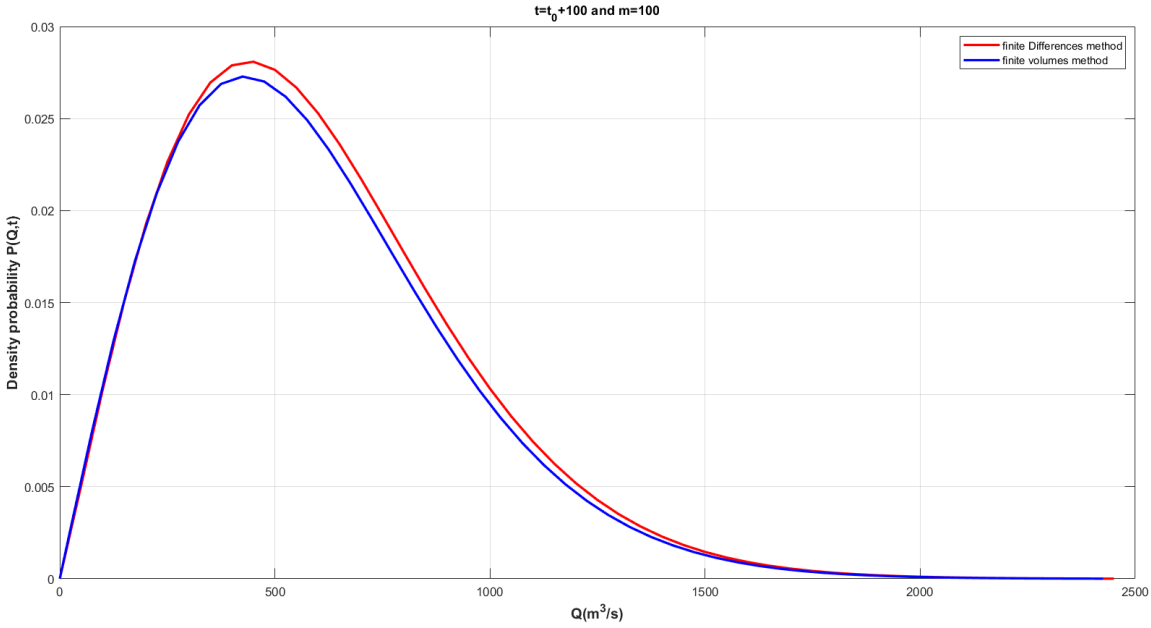

Figure 12. Comparison of the numerical solutions for m = 100 meshes.

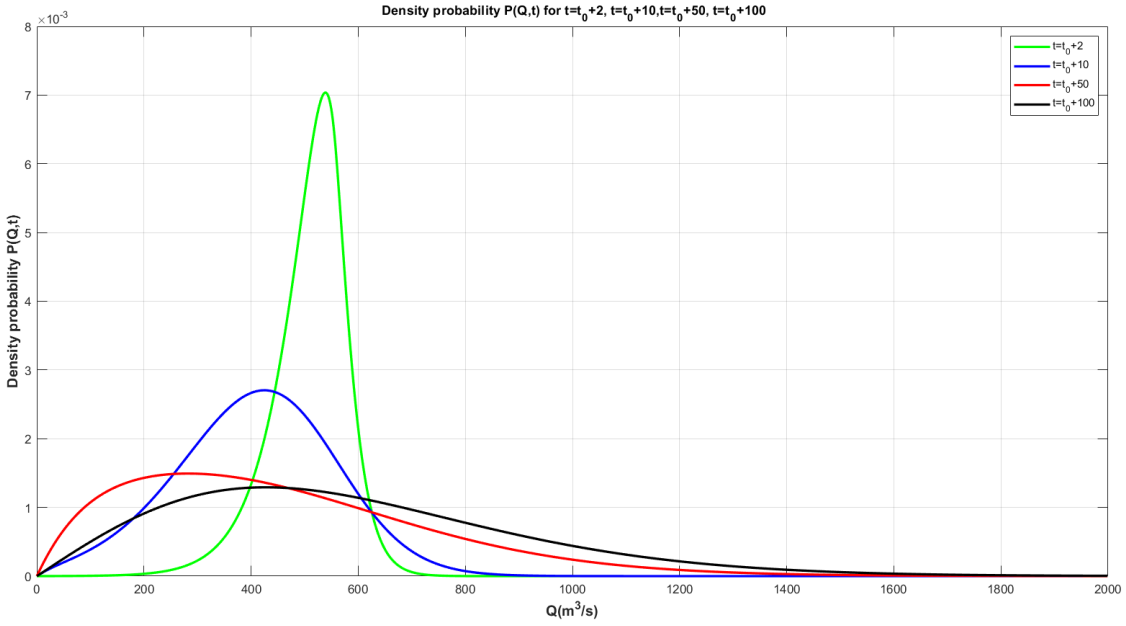

Figure 13. Density probability of discharge at $t_0 + 2$, $t_0 + 10$, $t_0 + 50$ *and* $t_0 + 100$ days.

the limits; this is due to the limit conditions. Figure 14 shows the evolution of density probability of discharge in the function of time and discharge. This confirms also the findings described in Figure 14. The above results are also in line with the findings of Biao et al. (2016) who used the Hermite orthogonal polynomial to approximate the exact solution of the FPE.

Using the initial discharge $Q_0 = 553.73\, m^3/s$ at date 22/07/2011 (t_0), one can derive the mean and the confidence interval (CI) at 90% around the mean discharge at day $t_0 + 10$ (Figure 15). We can derive that: CI = [144 and 637 m^3/s] and the mean = 410 m^3/s. So, there is 90% chance that the observed discharge of the day $t_0 + 10$ is between 144 and 637 m^3/s. The observed

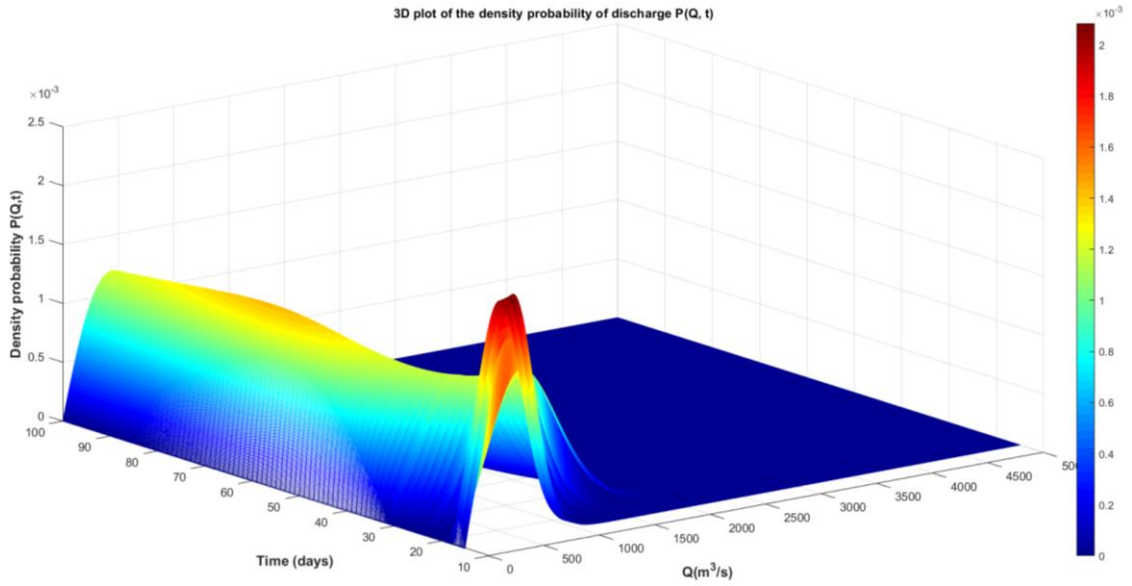

Figure 14. Three dimensional plot of the density probability of the discharges.

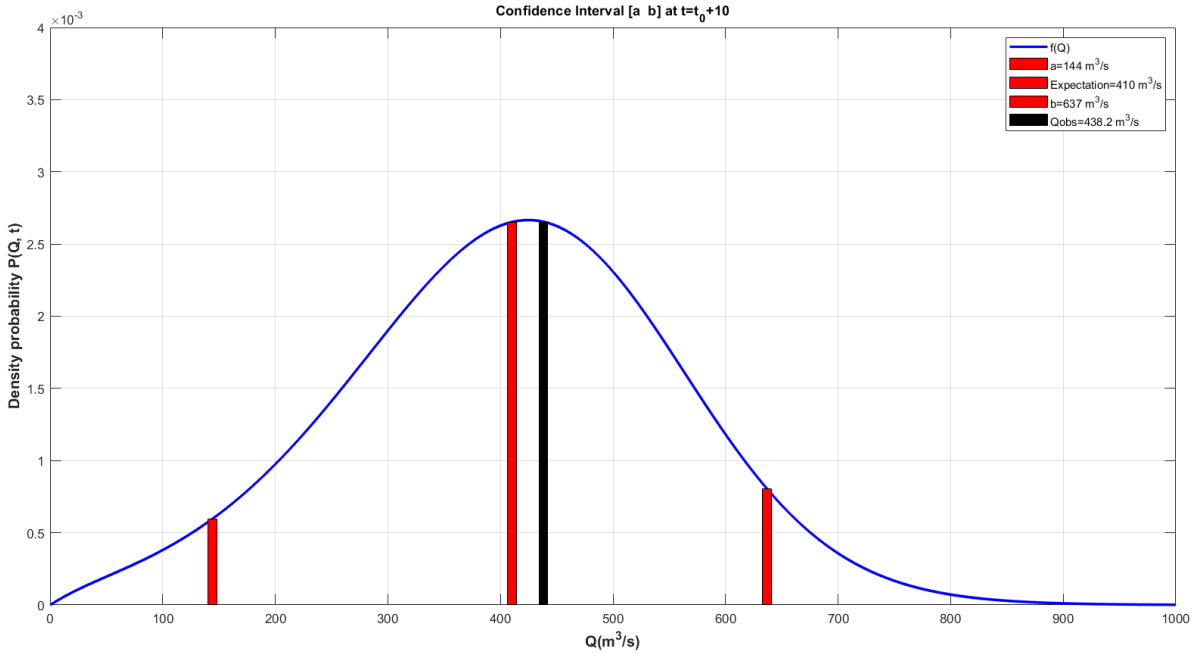

Figure 15. Confidence interval and the mean discharge at the date $t_0 + 10$.

discharge at the date $t_0 + 10$ is indeed within the confidence interval, close to the mean discharge. We can also calculate the probability that the discharge Q belongs to a given interval. For example $P(300 < Q < 550) = 0.602$. This means that there is a 60.2% chance that the discharge of the day belongs to the interval (300 and 550 m^3/s).

Conclusion

The main contribution of this paper was to use a stochastic approach to better account for both the dynamic and stochastic character of the hydrological phenomenon. The achievement of the objective of this paper stemmed from the combination of two modelling

approaches: first, deterministic modelling of the hydrological system by using ModHyPMA; and second, the stochastic formulation of ModHyPMA in terms of a stochastic differential equation (SDE). In comparison to the deterministic model, we discovered that the stochastic model improves simulations of discharge in the Ouémé at Savè Basin. The resolution of the Fokker Planck equation that is associated with the SDE was done using two different numerical methods: finite differences and finite volumes. The convergence of the two numerical methods investigated allows us to provide a solution that is close to the exact solution of the Fokker-Planck equation. This numerical solution can be used to calculate the uncertainty in the discharges in the Ouémé at Savè Basin. Although the use of the SDE and the associated FPE as proposed in this paper may become more complicated, the potential benefits in decision making, data collection, and information value are promising.

CONFLICT OF INTERESTS

The authors have not declared any conflict of interests.

ACKNOWLEDGEMENTS

The authors appreciate the researchers and institutions who provided datasets for this work, as well as Dr Adetola Jamal for his helpful suggestions. Thank you for the constructive comments and suggestions from the two anonymous reviewers.

REFERENCES

Afouda A, Alamou E (2010). Modèle hydrologique basé sur le principe de moindre action (MODHYPMA). Annales des Sciences Agronomiques du Bénin 13(1):23-45.

Afouda A, Lawin E, Lebel T (2004). A stochastic streamflow model based on a minimum energy expenditure concept. In contemporary problems in mathematical physics: Proceeding 3rd Intern Workshop. Word Scientific Publishing pp. 153-169.

Alamou E (2011). Application du principe de moindre action a la modélisation pluie – débit. Thèse de Doctorat. CIPMA – chaire UNESCO, Université d' Abomey Calavi.

Andréassian V, Perrin C, Parent E, Bárdossy A (2010). Editorial – The Court of Miracles of Hydrology: can failure stories contribute to hydrological science? Hydrological Sciences Journal 55(6):849-856.

Biao IE, Alamou AE, Afouda A (2016). Improving rainfall–runoff modelling through the control of uncertainties under increasing climate variability in the Ouémé River basin (Benin, West Africa), Hydrological Sciences Journal 61(16):2902-2915,

Bossa AY (2007). Modélisation du bilan hydrologique dans le bassin du Zou à l'exutoire d'Atchérigbé: contribution à l'utilisation durable des ressources en eau. Master thesis. Faculty of Agricultural Sciences, University of Abomey - Calavi, Benin.

Fallah NA, Bailey C, Cross M, Taylor GA (2000). Comparison of finite element and finite volume methods application in geometrically nonlinear stress analysis. Applied Mathematical Modelling 24(7):439-455.

Grossmann C, Roos HG, Stynes M (2007). Numerical Treatment of Partial Differential Equations. Springer Science & Business Media P 23. ISBN 978-3-540-71584-9.

Igué AM, Floquet A, Stahr K (2000). Land use and farming systems in Benin. In: Graef, F., P. Lawrence and M. von Oppen (Eds.): Adapted farming in West Africa: Issues, potentials and perspectives. Verlag Ulrich E. Grauer, Stuttgart, Germany. Stuttgart pp. 227-238.

IPCC (2014a). Climate Change 2014: Impacts, Adaptation, and Vulnerability. Part A: Global and Sectoral Aspects. Contribution of Working Group II to the Fifth Assessment Report of the Intergovernmental Panel on Climate Change [Field CB, VR. Barros, DJ. Dokken, KJ. Mach, MD. Mastrandrea, TE. Bilir, M. Chatterjee, KL. Ebi, YO. Estrada, RC. Genova, B. Girma, ES. Kissel, AN. Levy, S. MacCracken, PR. Mastrandrea, LL. White (eds.)]. Cambridge University Press, Cambridge, United Kingdom and New York, NY, USA 1132 p.

IPCC (2014b). Climate Change 2014: Impacts, Adaptation, and Vulnerability. Part B: Regional Aspects. Contribution of Working Group II to the Fifth Assessment Report of the Intergovernmental Panel on Climate Change [Barros VR., CB. Field DJ, Dokken MD, Mastrandrea KJ, Mach TE, Bilir M, Chatterjee KL, Ebi YO, Estrada RC, Genova B, Girma ES, Kissel AN, Levy S, MacCracken PR. Mastrandrea, LL. White (eds.)]. Cambridge University Press, Cambridge, United Kingdom and New York, NY, USA 688 p.

Kuczera G, Renard B, Thyer M, Kaveski D (2010). There are no hydrological monsters, just models and observations with large uncertainties! Hydrological Sciences Journal 55(6):980-991.

Kundzewicz ZW, Kanae S, Seneviratne SI, Handmer J, Nicholls N, Peduzzi P, Mechler R, Bouwer, LM, Arnell N, Mach K, Muir-Wood R, Brakenridge GR., Kron W, Benito G, Honda Y, Takahashi K, Sherstyukov B (2014). Flood risk and climate change: global and regional perspectives, Hydrological Sciences Journal 59(1):1-28.

Le Barbe L, Ale G, Millet B, Texier H, Borel Y, Gualde R (1993). Monographie des ressources en eaux superficielles de la République du Bénin. Paris, ORSTOM 540 p.

LeVeque R (2002). Finite Volume Methods for Hyperbolic Problems. ISBN 9780511791253.

Matheron G (1970). La théorie des variables régionalisées et ses applications. Les Cahiers du Centre de Morphologie Mathématique de Fontaine Bleau Fascicule 1:212.

Nash JE, Sutcliffe JV (1970). River flow forecasting through conceptual models part I – a discussion of principles. Journal of Hydrology 10(3):282-290.

Pauluhn A (1993). Stochastic beam dynamics in storage rings ; Thesis, DESY pp. 93-198.

Risken H (1989). The Fokker – Planck Equation. Methods of solution and applications. 2nd ed. Berlin: Springer – Verlag 472 p.

Sintondji LO, Zokpodo B, Ahouansou DM, Vissin WE, Agbossou K E (2014). Modelling the water balance of Ouémé catchment at the Savè outlet in Benin: contribution to the sustainable water resource management, International Journal of AgriScience 4(1):74-88.

Wojtkiewicz SF, Bergman LA, Spencer BF, Johson EA (1999). Numerical solution of the four-dimensional nonstatioanry Fokker-Planck equation. In IUTAM Symposium on Nonlinearity and Stochastic Structural Dynamics : proceedings of the IUTAM Symposium held in Madras, India, 4-8 January.

Zorzano MP, Mais H, Vazquez L (1999). Numerical solution of two dimensional Fokker-Planck equations. Applied mathematics and computation 98(2-3):109-117.